FORMATION OF ALUMINA-ALUMINIDE COATINGS ON FERRITIC-MARTENSITIC T91 STEEL

R.K. Choudhary [a] *, V. Kain [b], R.C. Hubli [a]

[a] Materials Processing Division, Bhabha Atomic Research Centre, Mumbai, India
[b] Materials Science Division, Bhabha Atomic Research Centre, Mumbai, India

Abstract

In this work, alumina-aluminide coatings were formed on ferritic-martensitic T91 steel substrate. First, coatings of aluminum were deposited electrochemically on T91 steel in a room temperature AlCl3-1-ethyl-3-methyl imidazolium chloride ionic liquid, then the obtained coating was subjected to a two stage heat treatment procedure consisting of prolonged heat treatment of the sample in vacuum at 300 °C followed by oxidative heat treatment in air at 650 °C for 16 hours. X-ray diffraction measurement of the oxidatively heat treated samples indicated formation of Fe-Al and Cr-Al intermetallics and presence of amorphous alumina. Energy dispersive X-ray spectroscopy measurement confirmed 50 wt-% O in the oxidized coating. Microscratch adhesion test conducted on alumina-aluminide coating formed on T91 steel substrate showed no major adhesive detachment up to 20 N loads. However, adhesive failure was observed at a few discrete points on the coating along the scratch track.

Keywords: alumina; aluminide; coating; electrodeposition; oxidation; adhesion

1. Introduction

Electrically insulative ceramic coatings are being proposed to minimize the magnetrohydrodynamic drag (MHD), prevent permeation of tritium through structural materials of the test blanket module (TBM) and also to protect the TBM steel against corrosion in molten Pb-Li coolant [1, 2]. The proposed coatings on the internal walls of TBM of fusion reactors are alumina stacked over Fe-Al based intermetallics. In this context, pack cementation and other methods have been explored to form alumina-aluminide coatings on ferritic-martensitic (F-M) steels [3, 4]. These F-M steels are being considered as a material of construction for TBM of fusion reactors. Besides the pack cementation and the other techniques, electrochemical methods are also being explored for this purpose [5, 6]. Aluminum coatings obtained by nonaqueous electrodeposition route, when converted to alumina-aluminide coatings by high temperature oxidation in air or controlled atmosphere are being considered for applications in fusion reactors [6]. For the past several years, ionic liquids have been used as a suitable nonaqueous electrolyte for aluminum electrodeposition [7−9]. However, only limited studies have been reported so far on alumina-aluminide formation by oxidation of aluminum coating. Also, physical, chemical and mechanical properties of these coatings need to be explored in detail to judge its suitability for use in fusion reactors.

Therefore in the present work, formation of alumina-aluminide coating by air oxidation of the electrodeposited aluminum from ionic liquids on ferritic-maretensitic T91 steel is studied. T91/P91 steel is a Fe9Cr1Mo ferritic-martensitic steel that finds major applications as structural material for various components in fusion reactors [10]. The so formed alumina-aluminide coating is evaluated in the present study for its adherence to the substrate by a microscratch adhesion testing technique. Possessing adequate adhesion to the substrate is a very important criterion for such coatings to be used in fusion reactors, as the coating must be able to withstand the shear force generated by the flowing liquid metal used as coolant for the fusion reactors. However, till date, no significant work is reported on the adhesion aspect for alumina-aluminide coatings formed on F-M steels.

2. Experimental
2.1 Materials

Aluminum coatings were electrodeposited both on mirror polished and wet alumina blasted T91 steel substrates (sample size: 25 mm x 20 mm x 2 mm) in a room temperature $AlCl_3$ (98%)-1-ethyl-3-methyl imidazolium chloride (EMIC, 98%) ionic liquid. High

* Corresponding author: rupeshkr@barc.gov.in

purity aluminum strips (purity: 99.95%, dimension: 150 mm x 25 mm x 2 mm) were used as anode.

2.2 Equipments

Electrodeposition was conducted in a custom designed glove box flushed with sufficient amount of high purity dry argon gas. A dry and inert atmosphere is essential for conducting electrodeposition of metals in ionic liquids since ionic liquids react readily with moisture and oxygen and becomes unusable [11]. Experiments were done in a 250 ml glass beaker. For carrying out the heat treatment of aluminum coated T91 steel, a programmable vacuum electric furnace was used. The samples were kept in an alumina crucible inside the furnace.

2.3 Procedure

Initially, a few electrodeposition experiments were attempted on mirror polished T91 steel substrate. However, due to inadequate adherence of the obtained coatings, the samples were not taken up for further studies. Subsequently, adherent aluminum coatings were successfully deposited on wet alumina blasted T91 steel substrates. Wet alumina blasting was done using pressurized alumina-water slurry having an average alumina particle size of 10 μm. Lewis acidic ionic liquid bath [12] was prepared by slowly mixing $AlCl_3$ powder with EMIC granules in a molar ratio of 2:1. Before coating, the substrate was immersed in a boiling 10 wt-% NaOH solution for 15 minutes followed by cleaning in dilute HCl solution to remove impurities. The cleaned substrate was dried with a hot air blower and weighed. There was no appreciable change in weight of the wet alumina blasted T91 steel substrate before and after cleaning and this ensured that the roughening caused due to wet alumina blasting was not affected by chemical cleaning. Prior to electrodeposition, the anodes were also cleaned in a 10 wt-% NaOH solution at 45 °C. Electrodeposition was conducted at 5, 7.5 and 10 mA cm^{-2} current densities for 2 hours in constant current mode. The current density values were obtained from literature [13].

After electrodeposition, aluminum coated T91 steel samples were subjected to a two stage heat treatment in a programmable electric furnace. First, aluminum coated sample was heated in vacuum (2.0 x 10^{-3} Pa) at a slow heating rate of 3 °C min^{-1} to a maximum temperature of 300 °C and then the sample was held at this temperature for more than 24 hours. In the second step, the adherent aluminum coatings were heated in a closed furnace in air at a relatively higher heating rate of 10 °C min^{-1} to 650 °C and soaked for 16 hours. The sample was cooled to room temperature at a very slow cooling rate of 2–3 °C min^{-1}.

2.4 Characterization of coating

X-ray diffraction (XRD) measurement was done for aluminum coatings before and after the heat treatment. XRD measurement was done in θ-2θ mode using monochromatized $Cu_{k\alpha}$ radiation at a wavelength of 0.154 nm. The obtained XRD pattern was matched with JCPDS database (card nos. 85-1327, 14-0336, 50-0955 and 02-1239) and peaks of aluminum, iron-aluminide and chromium-aluminide were identified. Diffusion of aluminum into T91 steel after first stage of heat treatment was confirmed by measuring composition of the sample by X-ray fluorescence (XRF) with top aluminum layer removed by mechanical polishing. Adhesion test was conducted for the coating after the heat treatment, using a software controlled microscratch adhesion tester in the progressive mode. In this scratch test, done as per ASTM standard C1624-05, the indenter is driven into the coating up to a maximum defined test load at a defined loading rate. Progressive mode scratch test is advantageous as it covers the full range of force. Therefore, in a single test, the load at which adhesive failure occurs in the coating can be determined. On the contrary, constant load scratch test requires a number of tests to confirm the load at which adhesive failure occurs in the coating. In the present work, during the scratch test a load of 0.9 N was applied at the start of the test whereas the maximum test load was 20 N at the end of the test. Parameters of the scratch tests are listed in Table 1. Normal load, frictional force and coefficient of friction, acoustic emission and depth of penetration data were recorded during the scratch test. The resulting scratch tracks left on the sample were examined under an optical microscope and the failure occurring in the sample was analyzed. Energy dispersive X-ray spectroscopy (EDS) measurement was done to analyze the composition of the as deposited and the oxidized samples. The oxidized samples were checked for electrical insulation by measuring electrical resistance

Table 1. *Scratch test parameters used in the present study.*

Parameters	Value
Load type	Progressive
Begin load	0.9 N
End load	20 N
Loading rate	30 N min^{-1}
Acoustic emission sensitivity	7
Indenter speed	4.71 mm min^{-1}
Scratch length	3 mm
Indenter type	Rockwell
Indenter material	Diamond
Indenter tip radius	200 μm

of the samples using a two probe electrical resistance measuring gauge. The average thickness of aluminum coatings was calculated from the weight gain after electrodeposition, assuming the density of aluminum coating to be same as that of bulk Al (2.7 g/cm^3).

3. Results and discussion

Figure 1a, 1b and 1c shows micrographs from scanning electron microscopic (SEM) examination of aluminum coating deposited on wet alumina blasted T91 steel substrate at 5, 7.5 and 10 mA cm^{-2} deposition current density, respectively. Formation of cellular microstructure with grains having the shape of a flake can be observed in Fig. 1a, whereas the

micrographs shown in Fig. 1b and 1c indicated formation of dense coatings. These features are more clearly shown in higher magnification micrographs in Fig. 1d, 1e and 1f for the coatings obtained at 5, 7.5 and 10 mA cm^{-2}, respectively.

The dense aluminum coating (thickness approximately 20 μm) obtained at 10 mA cm^{-2} was taken up for conversion to alumina by an oxidative heat treatment. However, due to large difference in coefficient of thermal expansion of aluminum and T91 steel it was difficult to obtain adherent oxidized aluminum coatings at a heat treatment temperature of 650 °C. A few single step heat treatment experiments conducted in air resulted in complete detachment of the coating from the substrate. Hence, the heat treatment
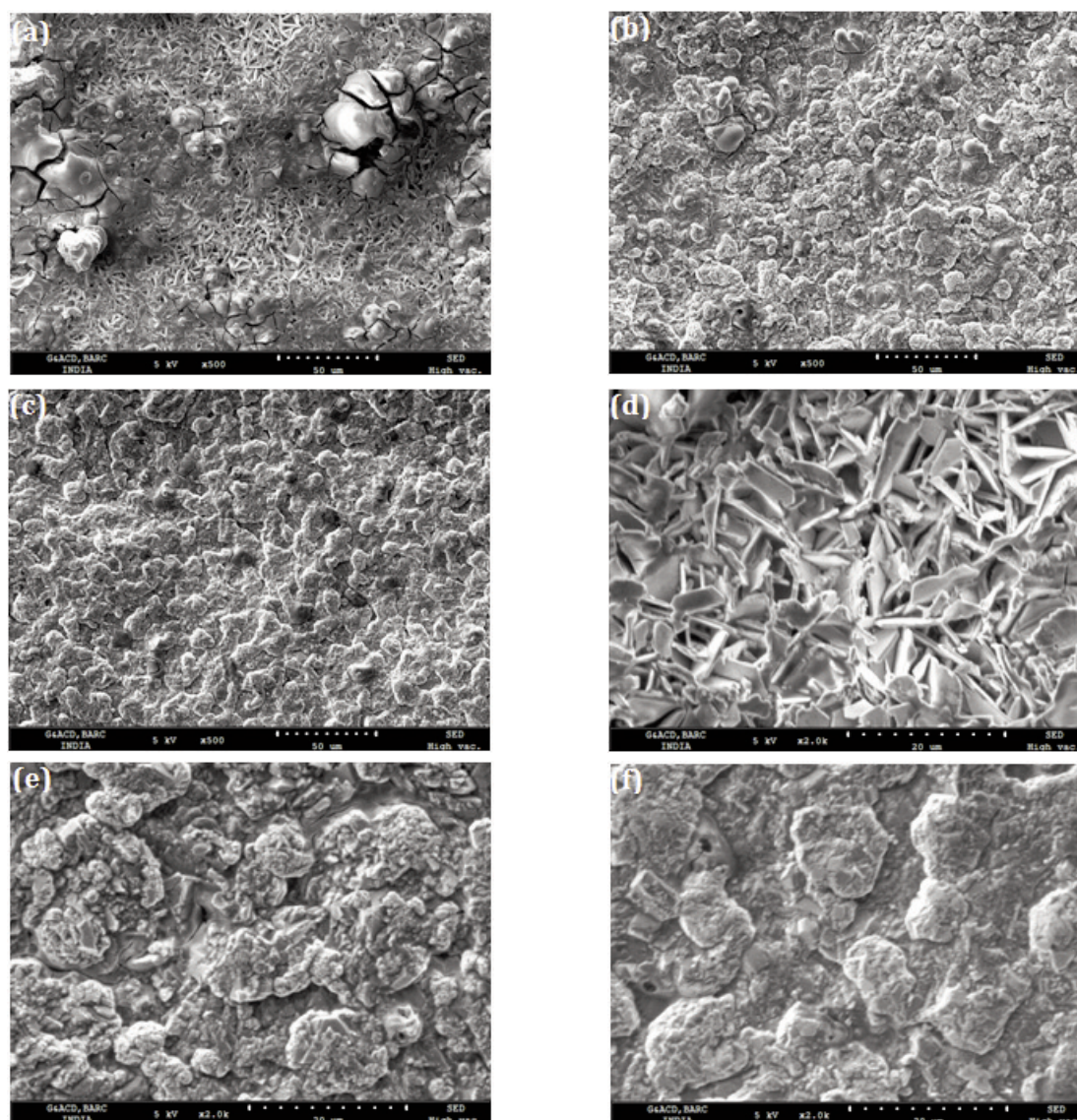

Figure 1. *SEM micrographs of aluminum coating deposited on T91 steel at (a) 5, (b) 7.5 and (c) 10 mA cm^{-2} current density. (d), (e) and (f) are higher magnification images of (a), (b) and (c) respectively.*

procedure was conducted in two steps as described in the experimental section. This process ensured improved bonding of aluminum coating with T91 steel due to diffusion of aluminum atoms into T91 steel. Diffusion of aluminum atoms into T91 steel was confirmed experimentally by removing the top aluminum layer formed on T91 steel by grinding and polishing and then measuring the composition of the sample by XRF. The chemical composition of this sample is presented in Table 2. It is clear that even after removal of aluminum coating completely from the substrate surface; atoms of aluminum still remained in T91 steel due to the diffusion that occurred during heat treatment. A higher heating rate was preferred in the second step of heat treatment since it favours the kinetics of conversion of aluminum to alumina [14]. Heat treatment was not attempted at temperatures higher than 650 °C since aluminum has a low melting temperature of 660 °C. The oxidized coatings were found to be electrically insulative as examined by measurement of electrical resistance.

Table 2. *Composition of T91 steel measured by XRF after removing the heat treated (up to 300 °C) Al coating.*

Element	Al	Si	P	V	Cr	Fe	Ni	Nb	Mo
Wt.%	9.09	0.35	0.17	0.131	6.04	82.63	0.11	0.075	0.819

XRD pattern of the as deposited and the heat treated aluminum coatings are shown in Fig. 2 (a). It is clear that even after the heat treatment, reflections of aluminum can be seen in the pattern, though the relative intensity of (111) and (200) reflections has changed. Besides this change, many new reflections were observed that appeared only after the heat treatment. These reflections are not very intense but clearly resolved, were found to be belonging to Fe-Al and Cr-Al based intermetallics. Konys *et al.* [5] reported formation of Fe-Al based intermetallics *e.g.* $FeAl_2$, FeAl, Fe_3Al and Fe_2Al_5 after annealing aluminum coating at 980 °C that was grown electrochemically on Eurofer 97 steel in ionic liquids. Similarly, Zhang *et al.* [6] also reported formation of Fe-Al intermetallics after a heat treatment at 700 °C.

In the XRD pattern (Fig. 2a), a crystalline phase of alumina could not be detected indicating that the so formed alumina was amorphous. This is also supported by the unresolved baseline of XRD pattern of the oxidized sample. There exists a large variation in the reported phases of alumina formed by air oxidation of aluminum. For instance, after air oxidation at 400 °C for 8 hours of aluminum coating electrodeposited on mild steel substrate in ionic liquids, Caporali *et al.* [15] reported formation of amorphous alumina films. However,

Zhang *et al.* [6] reported formation of γ-Al_2O_3 when aluminum coating electrodeposited in $AlCl_3$-EMIC ionic liquid on 321 stainless steel work piece was oxidized in a controlled atmosphere at 700 °C. Figures 2b and 2c show EDS patterns of the surface of the as deposited and the heat treated aluminum coatings, respectively. EDS measurement showed approximately 50 wt-% O present in the heat treated sample (Fig. 2c) whereas, no oxygen counts were observed in case of the as obtained deposit (Fig. 2b). EDS pattern also showed a small peak of chlorine which comes from the constituents of the bath ($AlCl_3$ or EMIC). However, EDS could not detect iron and chromium from Fe-Al and Cr-Al intermetallic phases respectively, which formed below the top alumina layer. This was due to interaction of electrons limited to a shorter distance in EDS measurement compared to deeper penetration of X-rays in XRD measurement. The optical micrograph of the cross-section of the oxidized coating showed nearly 20-30 μm thick aluminum rich coating formed on T91 steel (Fig. 2d).

Since the two step oxidative heat treatment was up to a maximum temperature of 650 °C, there was diffusion of aluminum into the substrate. The two step oxidation process resulted in conversion of the outer layer of aluminum coating to alumina. The same two step heating process also resulted in formation of intermetallics in the substrate region into which diffusion of aluminum had taken place (as shown in XRD pattern, Fig. 2a). The presence of reflections corresponding to aluminum (Fig. 2a) confirmed that aluminum was present in between the intermetallics (on the side of the substrate) and the outer alumina layer.

Figures 3a-h show the adhesion test results of oxidatively heat treated aluminum coating formed on T91 steel. The optical micrographs of the scratch tracks showed no major adhesive damage in the coating up to a maximum test load of 20 N. However, at a few locations on the scratch tracks, especially along the edges, adhesive failure or delamination was noticed (Fig. 3b-e) which may be due to insufficient diffusion of aluminum atoms occurring at such locations. Fig. 4 shows graphs of normal load and friction force, acoustic emission and penetration depth on the sample. Moreover, Fig. 4a shows large fluctuation in frictional force and coefficient of friction as the tip of the indenter progressed into the coating. This happened mainly due to higher roughness of the wet alumina blasted substrate. Moreover, in agreement with the adhesive failure observed along the scratch track there was appreciable acoustic emission in the form of sharp peaks detected by the acoustic sensor in the middle of the scratch track (Fig. 4b) and this
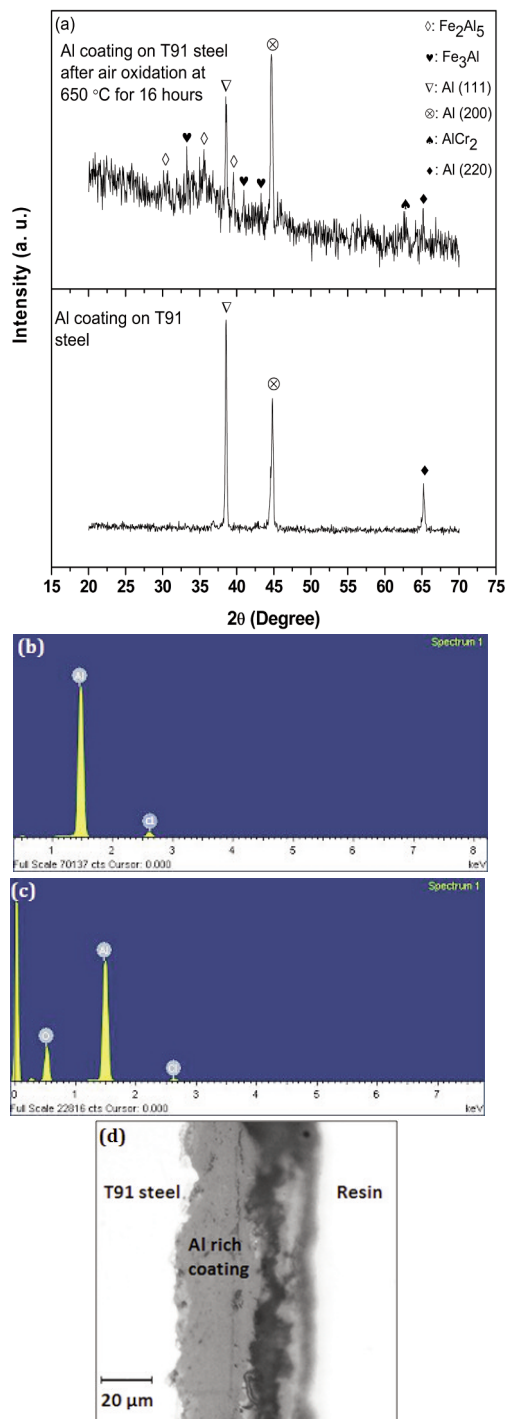
could indicate propagation of microcracks in the coating. The observed higher acoustic emission (Fig. 4b) was attributed to the spallation that occurred in the brittle alumina phase (formed during the oxidative heat treatment step). However, the acoustic emission decreased to a low constant value after the indenter tip attained a load of 14 N, in spite of the increase in tangential frictional force. It was attributed to the untransformed, ductile, aluminum that remained present below the top alumina layer. Presence of untransformed aluminum in the air oxidized sample is supported from (111), (200) and (220) reflections of Al observed in the XRD pattern (Fig. 2a). The load versus penetration curve shown in Fig. 4c did not show continuous increase in depth of penetration as the load increased progressively. This was again attributed to the uneven surface of the wet alumina blasted T91 steel substrate.
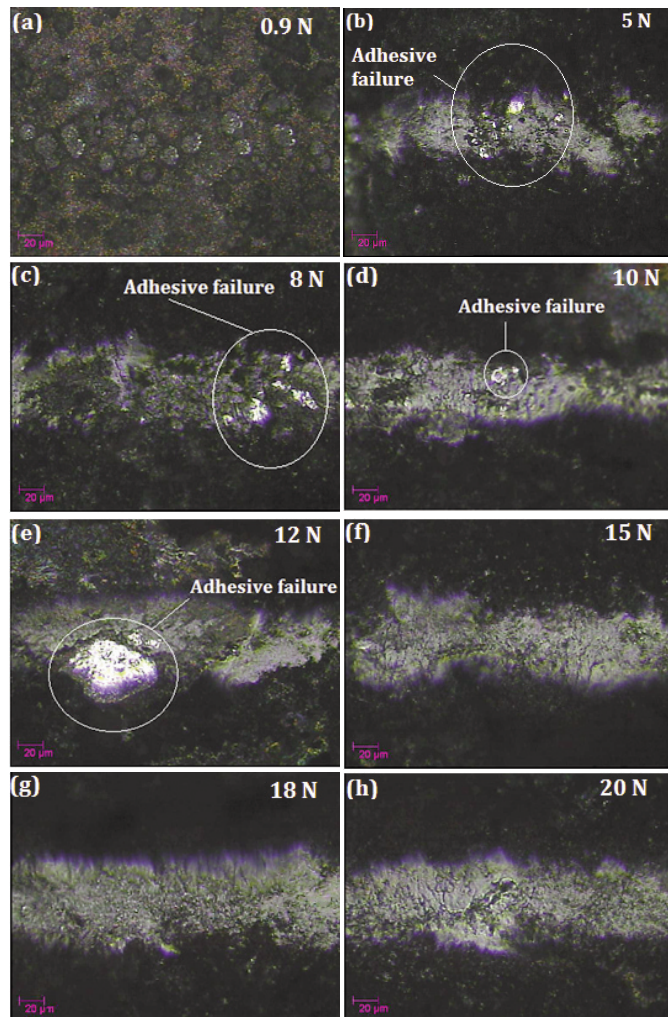

Figure 2. *(a) XRD pattern of aluminum coating as deposited on T91 steel and after oxidation in air at 650 °C for 16 hours, (b) EDS pattern of aluminum coating as deposited on T91 steel, (c) EDS pattern of aluminum coating deposited on T91 steel when subjected to oxidation in air at 650 °C for 16 hours and (d) cross-section optical micrograph of heat treated coating formed on T91 steel.*

Figure 3. *Optical micrographs of the scratch track left on air oxidized aluminum coating at different loads, after the adhesion test.*
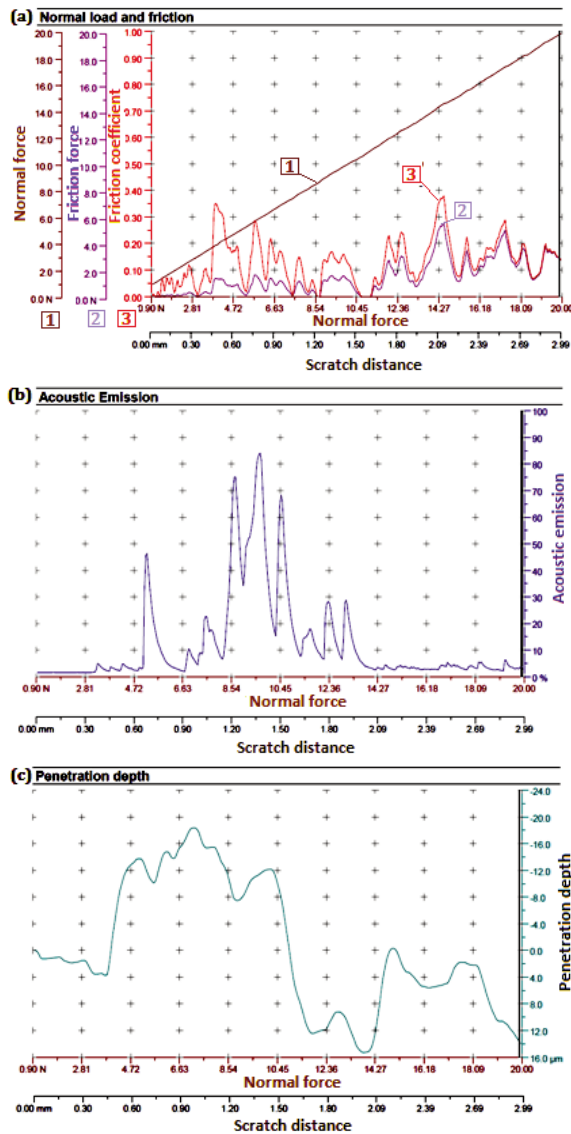
Figure 4. *(a) Normal load and friction, (b) acoustic emission and (c) penetration depth during adhesion test of air oxidized aluminum coating formed on T91 steel.*

4. Conclusions

Following conclusions are drawn from the present study:

1. Electrodeposition of aluminum in $AlCl_3$-EMIC ionic liquids followed by a two stage heat treatment resulted in formation of electrically insulative alumina coating on wet alumina blasted T91 steel. Adherent Al coatings could not be obtained on a mirror polished substrate.

2. Oxidative heat treatment of aluminum coating electrodeposited on T91 steel in air lead to its outer layer transforming to amorphous alumina.

3. Heat treatment during oxidation of aluminum coating electrodeposited on T91 steel in air lead to formation of Fe-Al and Cr-Al intermetallics by reaction with the substrate. These intermetallics were present at the substrate-Al interface, below the outermost alumina layer.

4. Heat treatment conducted in two steps lead to improved bonding of oxidized aluminum coatings with wet alumina blasted T91 steel substrate, which was otherwise not achieved during the single stage heat treatment.

References

[1] C.P.C. Wong, V. Chernov, A. Kimura, Y. Katoh, N. Morley, T. Muroga et al., J. Nucl. Mater., 367–370 (2007) 1287–1292

[2] D.L. Smith, J.H. Park, I. Lyublinski, V. Evtikhin, A. Perujo, H. Glassbrenner et al., Fusion Eng. Des., 61–62 (2002) 629–641.

[3] Y.Q. Wang, Y. Zhang, D.A. Wilson, Surf. Coat. Technol., 204 (2010) 2737–2744.

[4] N.I. Jamnapara, S. Frangini, D.U. Avtani, V.S. Nayak, N.L. Chauhan, G. Jhala, S. Mukherjee, A.S. Khanna, Surface Eng., 28 (2012) 700–704.

[5] J. Konys, W. Krauss, N. Holstein, Fusion Eng. Des., 85 (2010) 2141–2145.

[6] G.K. Zhang, C.A. Chen, D.L. Luo, X.L. Wang, Fusion Eng. Des., 87 (2012) 1370–1375.

[7] B. Li, C. Fan, Y. Chen, J. Lou, L. Yan, Electrochim. Acta, 56 (2011) 5478–5482.

[8] W. Huang, M. Wang, H. Wang, N. Ma, X. Li, Surf. Coat. Technol., 213 (2012) 264–270.

[9] M.H. Chuang, J.K. Chang, P.J. Tsai, W.T. Tsai, M.J. Deng, I.W. Sun, Surf. Coat. Technol., 205 (2010) 200–204.

[10] J.F. Salavy, G. Aiello, P. Aubert, L.V. Boccaccini, M. Daichendt, G.D. Dinechin et al., J. Nucl. Mater., 386–388 (2009) 922–926.

[11] Z. Liu, S. Zein El Abedin, F. Endres, Electrochim. Acta, 89 (2013) 635–643.

[12] Q.X. Liu, S. Zen El Abedin, F. Endres, J. Electrochem. Soc., 155 (2008) D357–D362.

[13] J. Tang, K. Azumi, Electrochim. Acta, 56 (2011) 1130–1137.

[14] S. Hasani, M. Panjepour, M. Shamanian, Open Access Scientific Reports, 1 (2012) 1–8.

[15] S. Caporali, A. Fossati, U. Bardi, Corros. Sci., 52 (2010) 235–241.